Ultrafast absorption recovery dynamics of 1300 nm quantum dot saturable absorber mirrors

M. P. Lumb, E. Clarke, E. Harbord, P. Spencer, R. Murray et al.

Citation: Appl. Phys. Lett. **95**, 041101 (2009); doi: 10.1063/1.3186081
View online: http://dx.doi.org/10.1063/1.3186081
View Table of Contents: http://apl.aip.org/resource/1/APPLAB/v95/i4
Published by the American Institute of Physics.

Ultrafast absorption recovery dynamics of 1300 nm quantum dot saturable absorber mirrors

M. P. Lumb,[1,a)] E. Clarke,[1] E. Harbord,[1] P. Spencer,[1] R. Murray,[1] F. Masia,[2] P. Borri,[2] W. Langbein,[2] C. G. Leburn,[3] C. Jappy,[3] N. K. Metzger,[3] C. T. A. Brown,[3] and W. Sibbett[3]
[1]*Department of Physics, Blackett Laboratory, Imperial College London, London SW7 2BW, United Kingdom*
[2]*School of Physics and Astronomy, University of Cardiff, Cardiff CF24 3AA, United Kingdom*
[3]*J. F. Allen Physics Research Laboratories, School of Physics and Astronomy, University of St. Andrews, Fife KY16 9SS, United Kingdom*

(Received 22 June 2009; accepted 1 July 2009; published online 27 July 2009)

We compare the performance of two quantum dot saturable absorber mirrors with one device operating at the quantum dot ground state transition whereas the other operates at the first excited state transition. Time-resolved photoluminescence and heterodyne four-wave mixing experiments demonstrate faster recovery of the excited-state device compared to the ground-state device. Femtosecond pulses were achieved with both devices, with the ground-state device producing 91 fs pulses and the excited-state device producing 86 fs pulses in a Cr:forsterite laser. The fast absorption recovery dynamics indicates the potential of devices exploiting excited-state transitions for use in high repetition rate lasers. © *2009 American Institute of Physics*. [DOI: 10.1063/1.3186081]

Semiconductor saturable absorber mirrors (SESAMs) are important elements in passively mode-locked lasers,[1] which are increasingly finding applications in medicine, telecommunications, and remote sensing. Recently, quantum dots (QDs) have been employed as the absorbing element, offering low saturation fluences, wide wavelength tunability (1–1.5 μm), broad inhomogeneous linewidths, and fast absorption recovery dynamics.[2–5] Fast recovery dynamics are helpful for forming and sustaining ultrashort pulses, and are necessary for efficient pulse formation in high repetition rate lasers.

We have recently demonstrated the first QD-SESAM device to operate with a QD excited state as the absorptive transition.[3] The higher degeneracy of the QD excited state offers larger absorption coefficients per dot layer compared to conventional ground state (GS) devices. Furthermore, faster absorption recovery is expected from excited states, reducing the need for postgrowth ion-implantation or low-temperature growth, both of which typically increase nonsaturable losses. However, a comparative study of the absorption recovery times of GS and excited state SESAM devices has not been undertaken. In the present work we make a direct comparison of two SESAM devices, one designed to operate in resonance with a GS transition (sample A) and the other in resonance with an excited state transition (sample B).

The devices are low-finesse, resonant structures [see Fig. 1(a)], incorporating nine absorbing QD layers in a resonant cavity with an optical thickness of $9\lambda_0/4$, where λ_0 is the design wavelength of 1290 nm. The QD layers are arranged in groups of three, separated by 40 nm spacer layers, centered at the antinodes of the electric field pattern at λ_0, calculated using a standard transfer matrix technique.

The QDs in sample A were grown by deposition of 2.4 ML of InAs at a rate of 0.014 ML^{-1} at a substrate temperature of T_S=485 °C and capped by 4 nm $In_{0.1}Ga_{0.9}As$ at T_S =470 °C, followed by 11 nm GaAs also grown at T_S =470 °C, with further GaAs grown at T_S=580 °C. This results in a QD density of 2.2×10^{10} cm^{-2} per layer (measured by atomic force microscopy of uncapped QDs grown under the same conditions) and peak room temperature GS emission at 1290 nm. The QDs in sample B are bilayers[6] consisting of an underlying seed layer separated by 10 nm of GaAs from a second QD layer. The seed layer was grown by deposition of 2.4 ML InAs at 0.014 ML^{-1} at a substrate temperature of 492 °C. The upper QD layer was grown by deposition of 3.3 ML InAs at T_S=467 °C also at 0.014 ML^{-1}, capped with 15 nm GaAs grown at T_S=467 °C and further

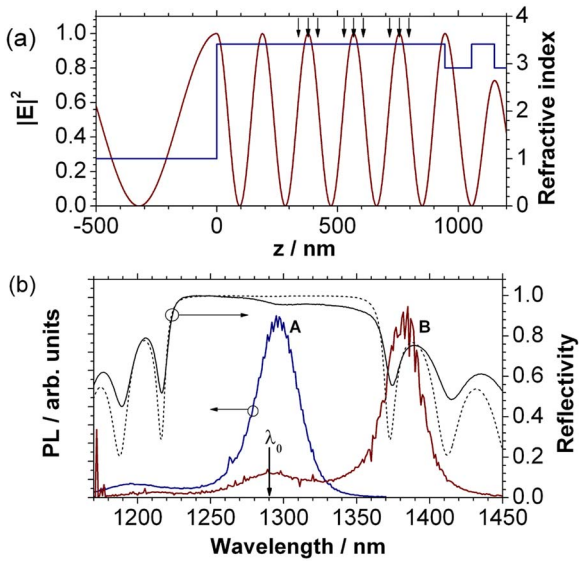

FIG. 1. (Color online) (a) The refractive index profile (blue) for the low-finesse, resonant SESAM with a $9\lambda_0/4$ cavity and the calculated field pattern at λ_0 (red). The arrows denote the position of the QD layers. (b) Room temperature PL spectra obtained from nominally identical samples of A and B, grown without the DBR. The dotted (full) line is the calculated (measured) reflectivity obtained from sample B. Noise around 1350–1400 nm is due to water absorption.

a)Electronic mail: matthew.lumb05@imperial.ac.uk.

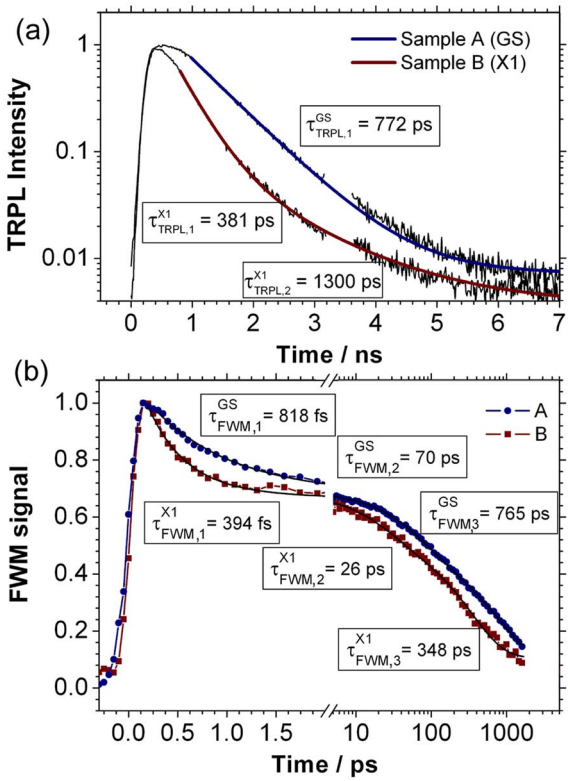

FIG. 2. (Color online) (a) Normalized, room temperature TRPL intensity for samples A and B at 1290 nm. (b) Room temperature FWM amplitude obtained at 1290 nm for samples A and B vs delay time t_{31}. Exponential fits and resulting decay times are indicated.

GaAs grown at T_S=580 °C. The areal density of the QDs in the second layer of the bilayer was 1.6×10^{10} cm^{-2}, slightly lower than for sample A due to the higher growth temperature of the seed layer. Emission from the GS of the second layer occurs at 1380 nm, with the first excited state (X1) emission at 1292 nm. Emission from the seed layer is suppressed, indicating an efficient carrier transfer to the second layer. The states of the seed layer QDs are at shorter wavelengths (around 1220 nm) and therefore do not participate in the absorption at λ_0. Room temperature photoluminescence (PL) spectra obtained from reference samples containing single layers of QDs grown under the same conditions as those in samples A and B (without the cavity structure) are presented in Fig. 1(b).

Figure 2(a) shows room temperature time-resolved PL measurements (TRPL) obtained from both samples using a time-correlated photon counting technique—nonresonant excitation by 3 ps pulses from a Ti:sapphire laser operating at 790 nm with a pulse fluence of around 400 μJ cm^{-2}. The luminescence decay from sample A is well described by a single exponential with a decay time of $\tau^{GS}_{TRPL,1}=772\pm2$ ps, while a biexponential decay consisting of a fast component of $\tau^{X1}_{TRPL,1}=381\pm3$ ps and a slower component of $\tau^{X1}_{TRPL,2}=1300\pm50$ ps was measured for sample B. The luminescence decay from sample B was dominated by the faster component, with the weighting factor of the fast component ~26 times larger than the slow component. Recent work by Harbord *et al.*[7] has attributed the fast component to luminescence from X1 states, and the slow component to a contribution from the GS of smaller QDs, which form a small proportion of the population of states resonant with 1290 nm. The faster luminescence lifetime of the excited state device is attributed to the increase in relaxation pathways for the carriers in the X1 state, via its increased degeneracy and fast relaxation to the GS,[8] and indicates the suitability of the excited state of QDs for application to high repetition rate laser systems. However as TRPL measures the overall decay of the carrier population following a complex scenario of nonresonant excitation, relaxation, and recombination, it is not sensitive to the fast resonant dynamics of a particular state. In order to probe the dynamics of carrier escape from the QD states on femtosecond timescales, a heterodyne four-wave mixing (FWM) experiment in resonance with the QD transition of interest was performed.[9,10]

In a three-beam transient FWM experiment, the sample is excited by three pulses which arrive at times 0, t_{21}, and t_{31}, respectively. The optical field E_1 of the first pulse generates a coherent polarization in the sample. If t_{21} is smaller than the dephasing time of the polarization, the field of the second pulse, E_2, produces a modulation of the exciton density ($\propto E_1^* E_2$) which evolves with the population dynamics. When the third pulse, E_3, arrives at the sample, a third-order polarization, i.e., FWM signal, ($\propto E_1^* E_2 E_3$) is induced in the sample, proportional to the remaining population modulation.

An optical parametric oscillator pumped by a femtosecond Ti:sapphire laser provided 150 fs Fourier-limited pulses at ν_0=76 MHz repetition rate, tunable from 1050 to 1600 nm wavelength with a spectral width of ~20 nm. In our heterodyne detection geometry three acousto-optic modulators (AOMs) are used to upshift the optical frequencies of $E_{1,2,3}$ by ν_1=80 MHz, ν_2=81.6 MHz, and ν_3=79 MHz, respectively. The three pulses are subsequently recombined with controlled delay times into the same spatial mode and focused on to the sample. The reflected fields and the nonlinear signal field are collected and interfere with a frequency-unshifted reference beam. A pair of balanced photodiodes detects the outgoing intensities and a lock-in amplifier discriminates the signal. The reflected fields and the emitted FWM signal can be distinguished by selecting the proper beating frequency as discussed in detail in Refs. 9 and 10. We chose the beating frequency to detect the reflected beams as the sideband of the AOM frequencies modulo the laser repetition rate, i.e., $\nu_{1(2)\{3\}}-\nu_0=4(5.6)\{3\}$ MHz, for E_1, E_2, and E_3, respectively, while $\nu_2-\nu_1+\nu_3-\nu_0=4.6$ MHz for the FWM signal. The dynamics of the transition resonant with the excitation were studied by exciting the sample with the first two pulses in time overlap (t_{21}=0) and measuring the dependence of the FWM amplitude on t_{31}.

The FWM field amplitude for samples A and B is displayed in Fig. 2(b). The data was obtained at 298 K using an excitation beam with 1290 nm central wavelength and an excitation density of 30 W/cm^2, giving an average pulse fluence of 0.4 μJ cm^{-2}. The measured data are fitted by a triexponential response, given by ($t>0.2$ ps)

$$\mathrm{FWM}(t)=A_{\mathrm{FWM},1}\exp\left[-\frac{t}{\tau_{\mathrm{FWM},1}}\right]+A_{\mathrm{FWM},2}\times\exp\left[-\frac{t}{\tau_{\mathrm{FWM},2}}\right]+A_{\mathrm{FWM},3}\exp\left[-\frac{t}{\tau_{\mathrm{FWM},3}}\right]+C. \quad (1)$$

TABLE I. Parameters for fit to FWM data for samples A and B.

Sample	Weighting factors			Time constants (ps)		
	$A_{\mathrm{FWM},1}$	$A_{\mathrm{FWM},2}$	$A_{\mathrm{FWM},3}$	$\tau_{\mathrm{FWM},1}$	$\tau_{\mathrm{FWM},2}$	$\tau_{\mathrm{FWM},3}$
A	0.402 ± 0.006	0.205 ± 0.008	0.378 ± 0.007	0.818 ± 0.02	70 ± 4	765 ± 59
B	0.504 ± 0.037	0.161 ± 0.01	0.417 ± 0.09	0.394 ± 0.03	26 ± 3	348 ± 20

Carriers can be removed from the absorbing state by a combination of carrier thermalization, escape, and interband recombination. The weighting factors of each mechanism are indicated by $A_{\mathrm{FWM},1-3}$. Table I compares the weighting factors and associated time constants for devices A and B. The proposed mechanism for the fast initial recovery decay is thermalization between the QD levels, mediated by phonons.[11] For carriers residing in the QD ground state, thermalization to a higher excited state can occur via absorption of phonons. However, carriers in the excited state can thermalize either by promotion to a higher excited state or relaxation to the ground-state via the spontaneous emission of phonons, leading to a more rapid decay. We tentatively assign the time constant measured at intermediate times to escape into the wetting layer. This is consistent with differential transmission measurements obtained from similar QDs in a waveguide structure, where absorption recovery on a <120 ps timescale was attributed to carrier escape from the QDs.[12] Clarifying this attribution shall be the attention of further study, including temperature and power dependencies. The final components of the decay are attributed to interband recombination, and these are in good agreement with the values of $\tau^{\mathrm{GS}}_{\mathrm{TRPL},1}$ and $\tau^{X1}_{\mathrm{TRPL},1}$ shown in Fig. 2(a). The factor of two reductions in the absorption recovery time for both the fast and slow components of the excited state transition absorption recovery is very important for several passive mode locking situations. The ultrafast thermalization of the excited state device is useful for ultrashort pulse generation and the faster overall density dynamics compared with the equivalent GS device offers the potential for higher pulse repetition rates to be attainable with the QD-SESAM.

Both devices were tested by inserting them into a Cr^{4+}:forsterite laser system, described in Ref. 13. These devices were capped with 190 nm MgO layers, which allows broadband elimination of group delay dispersion on reflection while maintaining low saturation fluence and a high modulation depth.[13] Laser operation using sample A supported pulses with a spectral bandwidth of 19.4 nm at a center wavelength of 1282 nm, giving a full width at half maximum pulse width of 91 fs, assuming sech^2 pulses. Sample B supported pulses with a spectral bandwidth of 20 nm at a center wavelength of 1280 nm. The time-bandwidth product was ≈ 0.33 in both cases, which implies near-transform-limited pulses. A maximum 55 mW of output power was generated for both devices. The performance of the two devices is therefore very similar, with both devices capable of supporting <100 fs pulses. However further optimization of the intracavity dispersion of the laser may produce shorter pulses still, and is subject to further study.

In conclusion, this result demonstrates that both ground and excited-state transitions of QDs in saturable absorber mirrors can be effectively used to produce femtosecond pulses. However, the different recovery channels of carriers resonantly excited into an excited-state leads to significantly faster absorption recovery. Therefore, ultrafast absorption recovery can be attained without the need for techniques such as postgrowth ion-implantation or low-temperature growth. This makes excited-state devices promising candidates for the production of ultrashort pulses at high repetition rates in a variety of systems over a wide wavelength range, and therefore demonstrates that the choice of QD transition is an important design consideration for QD-SESAMs.

F.M. is a European Union Marie Curie Fellow under Grant Agreement No. PIEF-GA-2008-220901. The dielectric capping was performed by Laseroptik GmbH.

[1] U. Keller, Nature (London) **424**, 831 (2003).
[2] D. J. H. C. Maas, A. R. Bellancourt, M. Hoffmann, B. Rudin, Y. Barbarin, M. Golling, T. Sudmeyer, and U. Keller, Opt. Express **16**, 18646 (2008).
[3] M. P. Lumb, D. J. Farrell, E. M. Clarke, M. J. Damzen, and R. Murray, Appl. Phys. B: Lasers Opt. **94**, 393 (2009).
[4] A. A. Lagatsky, F. M. Bain, C. T. A. Brown, W. Sibbett, D. A. Livshits, G. Erbert, and E. U. Rafailov, Appl. Phys. Lett. **91**, 231111 (2007).
[5] P. Borri, S. Schneider, W. Langbein, U. Woggon, A. E. Zhukov, V. M. Ustinov, N. N. Ledentsov, Z. I. Alferov, D. Ouyang, and D. Bimberg, Appl. Phys. Lett. **79**, 2633 (2001).
[6] E. C. Le Ru, P. Howe, T. S. Jones, and R. Murray, Phys. Rev. B **67**, 165303 (2003).
[7] E. Harbord, P. Spencer, E. Clarke, and R. Murray, J. Appl. Phys. **105**, 033507 (2009).
[8] S. Malik, E. C. Le Ru, D. Childs, and R. Murray, Phys. Rev. B **63**, 155313 (2001).
[9] P. Borri, W. Langbein, J. Mørk, and J. M. Hvam, Opt. Commun. **169**, 317 (1999).
[10] P. Borri and W. Langbein, J. Phys.: Condens. Matter **19**, 295201 (2007).
[11] R. Heitz, M. Veit, N. N. Ledentsov, A. Hoffmann, D. Bimberg, V. M. Ustinov, P. S. Kopev, and Z. I. Alferov, Phys. Rev. B **56**, 10435 (1997).
[12] D. B. Malins, A. Gomez-Iglesias, P. Spencer, E. Clarke, R. Murray, and A. Miller, Electron. Lett. **43**, 686 (2007).
[13] M. P. Lumb, P. N. Stavrinou, E. M. Clarke, R. Murray, C. G. L. Leburn, C. Jappy, N. K. Metzger, C. T. A. Brown, and W. Sibbett, Appl. Phys. B: Lasers Opt. (unpublished).